Article

Cell Reports

Bruton's Tyrosine Kinase Phosphorylates DDX41 and Activates Its Binding of dsDNA and STING to Initiate Type 1 Interferon Response

Graphical Abstract

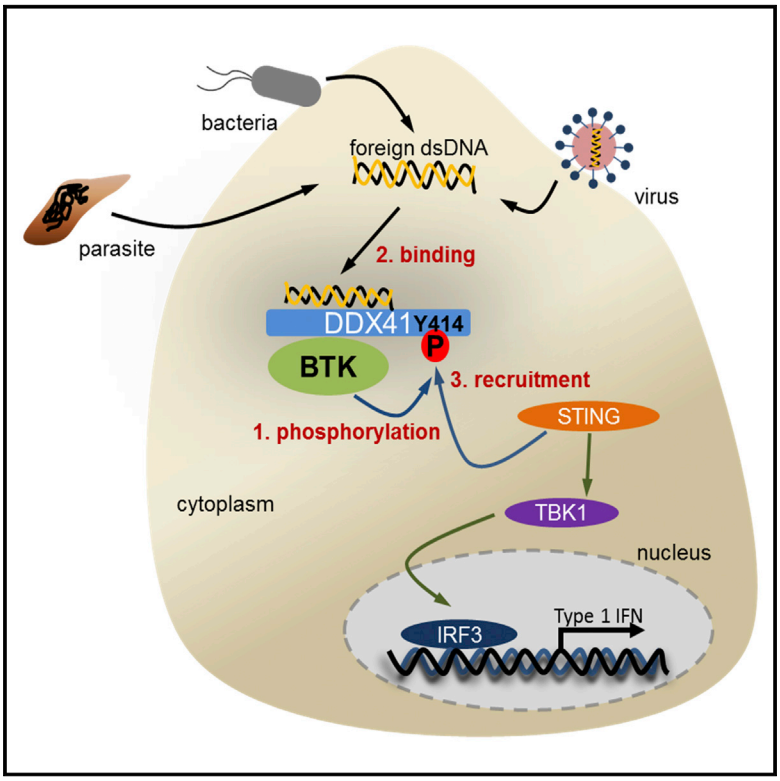

Authors

Koon-Guan Lee,
Susana Soo-Yeon Kim, ..., Yoshiaki Ito,
Kong-Peng Lam

Correspondence

lam_kong_peng@bti.a-star.edu.sg

In Brief

How DDX41 helicase functions as a DNA sensor is incompletely understood. Lee et al. find that BTK's kinase domain binds the DEAD-box domain of DDX41 and its SH3/SH2 interacting domain with STING's transmembrane region. BTK phosphorylates Tyr414 of DDX41 for foreign dsDNA recognition and recruitment of STING.

Highlights

- Induction of IFN-β by STING-activating agents is impaired in the absence of BTK
- BTK interacts with STING and the DNA sensor, DDX41 helicase
- BTK phosphorylates DDX41
- Tyr364 and Tyr414 of DDX41 are critical for DNA recognition and binding to STING

Lee et al., 2015, Cell Reports *10*, 1055–1065
February 24, 2015 ©2015 The Authors
http://dx.doi.org/10.1016/j.celrep.2015.01.039

Cell Reports
Article

Bruton's Tyrosine Kinase Phosphorylates DDX41 and Activates Its Binding of dsDNA and STING to Initiate Type 1 Interferon Response

Koon-Guan Lee,[1] Susana Soo-Yeon Kim,[1] Lin Kui,[1] Dominic Chih-Cheng Voon,[2] Marjorie Mauduit,[3] Pradeep Bist,[4] Xuezhi Bi,[1] Natasha Ann Pereira,[1] Chengcheng Liu,[1] Bindu Sukumaran,[4] Laurent Rénia,[3] Yoshiaki Ito,[2] and Kong-Peng Lam[1,5,*]

[1]Bioprocessing Technology Institute, Agency for Science, Technology and Research, Singapore 138668, Singapore
[2]Cancer Biology Program, Cancer Science Institute, National University of Singapore, Singapore 117599, Singapore
[3]Singapore Immunology Network, Agency for Science, Technology and Research, Singapore 138648, Singapore
[4]Emerging Infectious Diseases Program, DUKE-NUS Graduate Medical School, Singapore 169857, Singapore
[5]Departments of Microbiology, Physiology, and Paediatrics, Yong Loo Lin School of Medicine, National University of Singapore, Singapore 117574, Singapore
*Correspondence: lam_kong_peng@bti.a-star.edu.sg
http://dx.doi.org/10.1016/j.celrep.2015.01.039

SUMMARY

The innate immune system senses cytosolic dsDNA and bacterial cyclic dinucleotides and initiates signaling via the adaptor STING to induce type 1 interferon (IFN) response. We demonstrate here that BTK-deficient cells have impaired IFN-β production and TBK1/IRF3 activation when stimulated with agonists or infected with pathogens that activate STING signaling. BTK interacts with STING and DDX41 helicase. The kinase and SH3/SH2 interaction domains of BTK bind, respectively, the DEAD-box domain of DDX41 and transmembrane region of STING. BTK phosphorylates DDX41, and its kinase activities are critical for STING-mediated IFN-β production. We show that Tyr364 and Tyr414 of DDX41 are critical for its recognition of AT-rich DNA and binding to STING, and tandem mass spectrometry identifies Tyr414 as the BTK phosphorylation site. Modeling studies further indicate that phospho-Tyr414 strengthens DDX41's interaction with STING. Hence, BTK plays a critical role in the activation of DDX41 helicase and STING signaling.

INTRODUCTION

The innate immune system detects pathogen-associated nucleic acids via pattern-recognition receptors (PRRs) and initiates type 1 interferon (IFN) production (Takeuchi and Akira, 2009). Toll-like receptors (TLRs) recognize foreign DNA and RNA on cell surfaces and in endosomes (Blasius and Beutler, 2010), while DAI (Takaoka et al., 2007), AIM2 (Hornung et al., 2009), IFI16 (Unterholzner et al., 2010), cGAS (Sun et al., 2013; Diner et al., 2013; Ablasser et al., 2013), and the DEAD (aspartate-glutamate-alanine-aspartate)-box helicase DDX41 (Zhang et al., 2011) sense foreign nucleic acids in the cytosol.

DDX41 is ubiquitously expressed and detects not only viral double-stranded (ds) DNA but also bacterial cyclic dinucleotides (CDNs) such as cyclic di-AMP and cyclic di-GMP (Parvatiyar et al., 2012). CDNs are second messengers that regulate the motility and virulence of microbes and are not produced by mammalian cells (Mills et al., 2011). Hence, their presence activates the host response. DDX41 directly binds dsDNA (Zhang et al., 2011) and CDNs (Parvatiyar et al., 2012) and associates with the adaptor STING (stimulator of IFN genes) to activate TBK1, which phosphorylates the transcription factor IRF3 to trigger IFN production. STING resides in the endoplasmic reticulum but relocates upon activation to cytosolic punctuate structures to nucleate the formation of an IFN-inducing signalosome (Ishikawa et al., 2009).

DDX41 possesses a helicase and a DEAD-box domain that binds dsDNA, CDNs, and STING (Zhang et al., 2011; Parvatiyar et al., 2012). Recruitment of STING to DDX41 is activated by ligand binding to DDX41. After activation, DDX41 undergoes K48-linked ubiquitination by TRIM21 that leads to its degradation and termination of the innate response (Zhang et al., 2013).

The exact mechanism of how DDX41 functions as a PRR remains unclear. In mouse cells, DDX41 and STING co-precipitated in a ligand-dependent manner (Zhang et al., 2011), suggesting that STING binds to DDX41 only upon engagement. It is not known whether any protein modification is required for DDX41 activation and how DDX41 couples to STING after ligand sensing. It is also unclear whether other signaling molecule is involved in DDX41 activation.

Bruton's tyrosine kinase (BTK) belongs to the Tec family of cytoplasmic tyrosine kinases and plays a role in B cell receptor signaling and lymphopoiesis (Khan et al., 1995). Its mutations lead to *X-linked agammaglobulinemia* in human and *X-linked immunodeficiency* in mice. It also has a role in TLR signaling (Jefferies et al., 2003; Liljeroos et al., 2007; Lee et al., 2008). BTK binds TLR2, 6, 8, and 9 (Horwood et al., 2006; Doyle

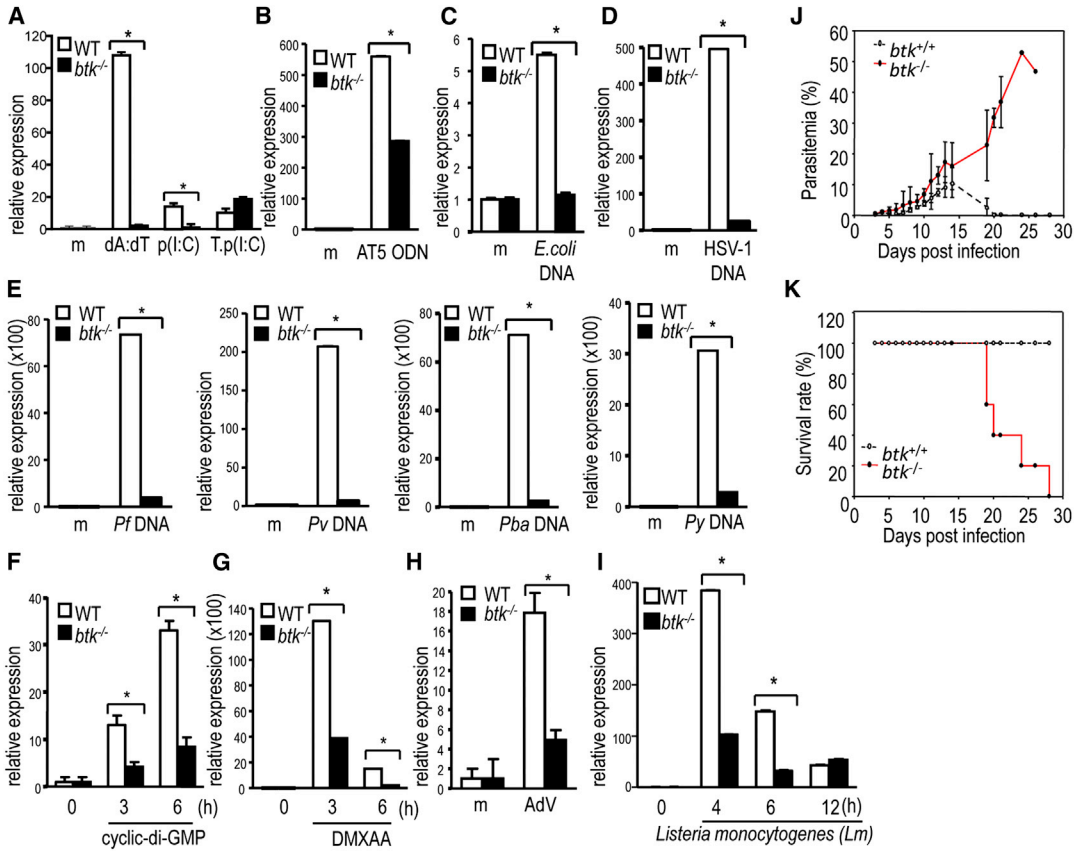

Figure 1. BTK Is Required for *ifnb* mRNA Induction by STING-Activating Stimuli

(A) Real-time RT-PCR quantification of *ifnb* mRNA in (A) WT and $btk^{-/-}$ MEF transfected with p(dA:dT) or p(I:C) in LyoVec (T.p(I:C)) or stimulated exogeneously with naked p(I:C) for 6 hr.

(B–D) WT and $btk^{-/-}$ bone marrow-derived macrophages (BMDMs) treated for 6 hr with AT5-ODN (B), *E. coli* DNA (C), or HSV-1 DNA (D).

(E) WT and $btk^{-/-}$ MEF stimulated for 6 hr with DNA from human and murine malaria parasites, including *Plasmodium falciparum* (*Pf*), *Plasmodium vivax* (*Pv*), *Plasmodium berghei ANKA* (*Pba*), and *Plasmodium yoelii* (*Py*).

(F and G) WT and $btk^{-/-}$ BMDMs transfected with bacterial cyclic di-GMP (F) or stimulated with DMXAA (G) for 3 to 6 hr.

(H and I) WT and $btk^{-/-}$ BMDMs infected with adenovirus (H) or *Listeria monocytogenes* (I) for 6 hr.

(J and K) Parasitemia (J) and survival (K) of WT and $btk^{-/-}$ mice infected with *P. yoelii* (1×10^6 infected red blood cell). Data shown are representative of three independent experiments; *$p < 0.05$.

See also Figures S1 and S2.

et al., 2007) and MyD88 and TRIF adaptors (Liu et al., 2011). It also phosphorylates the Mal adaptor involved in TLR4 signaling (Gray et al., 2006) and TLR3 (Lee et al., 2012). However, it is not known whether BTK participates in STING signaling.

Here, we show that BTK plays a critical role in STING-mediated sensing of cytosolic dsDNA and bacterial CDNs. BTK-deficient cells were impaired in IFN-β production when treated with dsDNA, CDNs, DMXAA, or AT-rich *plasmodium* DNA or infected with *listeria monocytogenes* and adenoviruses. BTK physically binds STING and DDX41, and we identify the domains critical for BTK-STING and BTK-DDX41 interactions. We further demonstrate that BTK phosphorylates DDX41 and more importantly that DDX41 binding of dsDNA and STING are activated by protein tyrosine phosphorylation, and we identify the critical tyrosine residue involved.

RESULTS

A Role for BTK in STING-Mediated Signaling

To test whether BTK participates in innate sensing of dsDNA, we transfected WT and $btk^{-/-}$ murine embryonic fibroblasts (MEFs) with synthetic B-form dsDNA (p(dA:dT)) or liposome-enclosed p(I:C) or stimulated them exogeneously with naked p(I:C) as control and measured their *ifnb* mRNA synthesis via real-time RT-PCR. We found $btk^{-/-}$ MEF to produce significantly less *ifnb* mRNA compared with WT cells when they were transfected with p(dA:dT) but not p(I:C) (Figure 1A). They also had reduced induction of IFN-responsive genes such as *isg56*, *isg15*, *cxcl10*, and NFκB-dependent genes such as *il6* (Figures S1A–S1D). As p(dA:dT) can be transcribed by RNA polymerase III into RNA that stimulates cytosolic RNA sensor RIG-I and its downstream adaptor IPS-1 (Ablasser et al., 2009; Chiu et al., 2009) and since

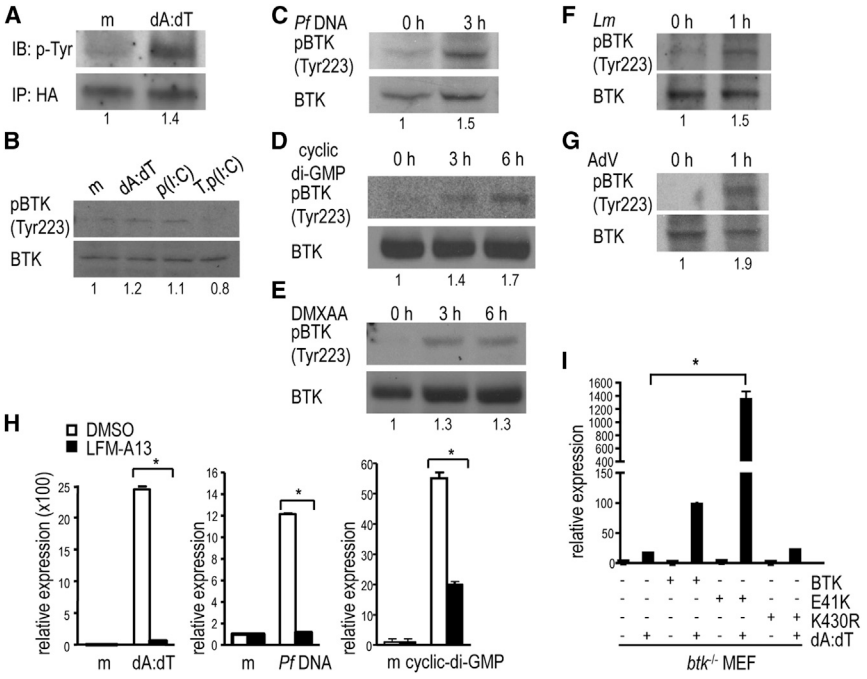

Figure 2. BTK Is Phosphorylated, and Its Kinase Activity Is Required during STING Signaling

(A) WT MEF transfected with HA-BTK plasmids were nontreated (m) or transfected with p(dA:dT)/LyoVec for 1 hr. BTK was immunoprecipitated (IP) with anti-HA antibody and immunoblotted (IB) with anti-phosphotyrosine (pTyr) antibody. The anti-HA blot served as loading control.

(B) WT macrophages were nontreated (m), transfected with p(dA:dT) or p(I:C) in LyoVec (T.p(I:C)), or stimulated extracellularly with p(I:C) for 1 hr and examined for BTK activation using anti-phospho-BTK (Tyr223) antibody. The anti-BTK blot served as loading controls.

(C–G) WT BMDMs were stimulated with *Plasmodium falciparum* DNA (*Pf*; C), cyclic di-GMP (D), DMXAA (E), or infected with *listeria monocytogenes*, MOI = 1 (F), or adenovirus (G). Cell lysates were examined using anti-phospho-BTK (Tyr223) antibody.

(H) BTK kinase activity is critical for STING-mediated *ifnb* mRNA synthesis. WT MEF were pretreated with DMSO or BTK inhibitor LFM-A13 for 1 hr and transfected with p(dA:dT)/LyoVec, *Pf* DNA, or cyclic di-GMP for 6 hr and *ifnb* mRNA synthesis quantified via real-time RT-PCR.

(I) *btk*$^{-/-}$ MEF infected with retrovirus bearing WT, constitutive-active (E41K), or kinase-dead (K430R) BTK were nontreated or transfected with p(dA:dT) for 6 hr and *ifnb* mRNA induction quantified via real-time RT-PCR. Data shown are representative of three independent experiments; *p < 0.05. Densitometry was performed on western blot images, and numerical values normalized and compared with nonstimulated sample are indicated below each corresponding lane. See also Figure S3.

BTK is also known to be involved in dsRNA recognition specifically via TLR3 but not RIG-I (Lee et al., 2012), we next challenged WT and *btk*$^{-/-}$ cells with an AT-rich synthetic oligonucleotide (AT5-ODN) that bears a secondary stem-loop structure and shown previously to induce IFN-β production in a IPS-1- or TLR-independent manner (Sharma et al., 2011). Again *btk*$^{-/-}$ cells were impaired in *ifnb* mRNA expression compared with WT cells (Figure 1B). These data suggest that BTK is involved in host response to pathogenic cytosolic dsDNA. Consistent with this hypothesis, *btk*$^{-/-}$ MEF had defective *ifnb* mRNA synthesis when transfected with *E. coli* (Figure 1C) or HSV-1 (Figure 1D) DNA. Similarly, *btk*$^{-/-}$ MEF were unable to produce *ifnb* mRNA when challenged with AT-rich DNA derived from various strains of human or mouse malaria parasites (Figure 1E).

AT5-ODN, HSV-1, and malarial DNA trigger IFN-β production via STING (Ishikawa et al., 2009; Sharma et al., 2011). To examine whether BTK is involved in this pathway, we stimulated WT and *btk*$^{-/-}$ cells with bacterial second messenger cyclic-di-GMP (Figure 1F) and chemotherapeutic agent 5,6-dimethylxanthenone-4-acetic acid (DMXAA) (Figure 1G), both of which activate STING signaling (Prantner et al., 2012). Interestingly, *btk*$^{-/-}$ cells also could not synthesize *ifnb*, *isg56*, *isg15*, and *mx1* mRNAs (Figures S1E–S1I) when exposed to these stimulants.

To assess the physiological relevance of these findings, we infected WT and *btk*$^{-/-}$ macrophages with adenovirus (Figure 1H) or *Listeria monocytogenes* (Figure 1I) that were known to trigger STING signaling (Ishikawa et al., 2009; Stein et al., 2012) and showed that *btk*$^{-/-}$ cells had impaired *ifnb* mRNA synthesis when challenged with these pathogens. *Listeria*-infected *btk*$^{-/-}$ macrophages also had defective *isg56* mRNA synthesis (Figure S1J). The role of BTK in DNA sensing via STING appeared specific as *btk*$^{-/-}$ macrophages infected with influenza virus had normal production of *ifnb*, *isg56*, and *isg15* mRNAs (Figures S2A–S2C), as this RNA virus triggered innate response via IPS-1 (Opitz et al., 2007).

We next infected WT and *btk*$^{-/-}$ mice with *Plasmodium yoelii* and monitored their parasitemia (Figure 1J) and survival (Figure 1K). Infected *btk*$^{-/-}$ mice developed more severe parasitemia and manifested greater mortality. In contrast, WT mice could clear parasites and survived. These data were consistent with a role for BTK in innate sensing of AT-rich DNA (Figure 1E).

BTK Activity Is Required for STING Signaling

BTK is tyrosine phosphorylated upon activation (Lee et al., 2008; Matsuda et al., 1995; Sato et al., 1994). We next asked whether BTK was phosphorylated in cells stimulated with STING-activating agents. We showed that both exogenously overexpressed (Figure 2A) and endogenous (Figure 2B) BTK were phosphorylated in p(dA:dT)-transfected MEF and macrophages. As controls, we showed that BTK was phosphorylated in cells stimulated with naked p(I:C) that activated TLR3 but not in cells transfected with liposome-enclosed p(I:C) that activated RIG-I (Figure 2B) (Onomoto et al., 2007). BTK was also phosphorylated when macrophages were transfected with AT-rich DNA from *plasmodium falciparum* (Figure 2C) and bacterial cyclic-di-GMP (Figure 2D), treated with DMXAA (Figure 2E), or infected with *listeria monocytogenes* (Figure 2F) and adenovirus (Figure 2G), but not when they were infected with influenza virus that activated IPS-1 (Figure S3A).

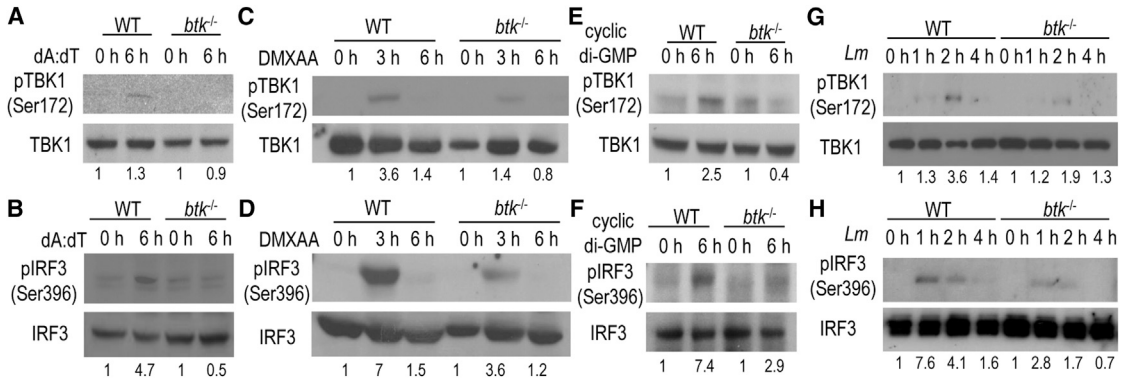

Figure 3. BTK Deficiency Impairs STING-Mediated TBK1 and IRF3 Activation

(A–H) WT and *btk*$^{-/-}$ BMDMs were stimulated with p(dA:dT) (A and B), DMXAA (C and D), and cyclic di-GMP (E and F) or infected with *listeria monocytogenes* MOI = 1 (G and H). Cell lysates were examined via western blotting with anti-phospho-TBK1 (Ser172) (A, C, E, and G) and anti-phospho-IRF3 (Ser396) (B, D, F, and H) antibodies. Anti-TBK1 and anti-IRF3 blots served as loading controls. Densitometry readings are provided as in Figure 2.

As BTK is a multidomain protein with adaptor and tyrosine kinase functions (Mohamed et al., 2009), we treated WT cells with the chemical inhibitor LFM-A13 and assessed their synthesis of *ifnb* mRNA in response to p(dA:dT), malaria DNA, or bacterial cyclic-di-GMP. Our data indicated that BTK-inhibited cells were defective in producing *ifnb* (Figure 2H) and *il6* (Figure S3B) mRNAs when challenged with these agents, suggesting that BTK tyrosine kinase activity is important for STING signaling.

To confirm that BTK kinase activity is critical for *ifnb* mRNA induction in response to STING-activating agents, we introduced WT, constitutive-active (E41K), or kinase-dead (K430R) BTK into *btk*$^{-/-}$ MEF and stimulated them with p(dA:dT). We found *ifnb* mRNA synthesis to be restored in mutant cells transduced with WT BTK (Figure 2I), significantly enhanced in cells harboring E41K-BTK, but defective in cells bearing K430R-BTK. These data indicated that BTK is phosphorylated and its kinase activity is required for STING signaling.

BTK Deficiency Impairs STING-Mediated TBK1 and IRF3 Activation

STING-signaling activates TBK1, which phosphorylates the IRF3 transcription factor that induces *ifnb* mRNA synthesis (Barber, 2011). We next examined the effect of BTK-deficiency on TBK1 and IRF3 activation. Western blot analyses using anti--phospho-TBK1 and anti-phospho-IRF3 antibodies indicated that *btk*$^{-/-}$ macrophages were defective in TBK1 (Figure 3A) and IRF3 (Figure 3B) activation when they were transfected with p(dA:dT). Mutant cells stimulated with DMXAA (Figures 3C and 3D), transfected with bacterial cyclic di-GMP (Figures 3E and 3F), or infected with *listeria monocytogenes* (Figures 3G and 3H) also had impaired TBK1 and IRF3 phosphorylation. Hence, BTK deficiency compromises TBK1 and IRF3 activation, suggesting that BTK plays a pivotal role and acts upstream of these molecules in STING signaling.

BTK Interacts with STING

To gain insight to BTK's role in STING signaling, we overexpressed BTK and various mutants alone or with STING in HEK293T cells and examined the induction of *ifnb* promoter activity using a luciferase-based reporter assay (Figure 4A). We found substantial induction of *ifnb* promoter activity when STING and BTK were co-expressed, suggesting that they acted in concert to drive *ifnb* mRNA synthesis. Overexpression of constitutive-active BTK (E41K) further synergizes with STING to induce *ifnb* promoter activity, whereas overexpression of kinase-dead BTK (K430R) did not. This study confirms that BTK and its kinase activity are critically important for STING signaling.

Since BTK deficiency impaired activation events downstream of STING (Figure 3) and TBK1 complex with STING upon activation (Tanaka and Chen, 2012), we investigated whether BTK could directly bind STING. We overexpressed HA-tagged STING or IPS-1 (as negative control) with FLAG-tagged BTK in HEK293T cells and showed that BTK co-immunoprecipitated with STING but not with IPS-1 (Figure 4B). We confirmed the specificity of our reagents and showed that the tagged proteins could not be immunoprecipitated with control IgG antibodies (Figure S4A). The BTK and STING interaction was further supported by confocal microscopy studies showing that the two molecules co-localized when they were overexpressed in HEK293T cells (Figure 4C). BTK and STING were also found to interact endogenously in WT macrophages transfected with p(dA:dT) (Figure 4D). As BTK kinase activity is critical for STING signaling, we test whether BTK could phosphorylate STING. However, STING was not phosphorylated when overexpressed with constitutive-active BTK (Figure S4B). Hence, our data indicated that BTK physically binds but does not phosphorylate STING. We also showed that BTK could interact with the E3-ubiquitin ligase TRIM56 (Figure S4C), which is part of the STING signalosome (Tsuchida et al., 2010) but could not phosphorylate it (Figure S4D).

BTK Directly Binds and Phosphorylates DDX41 Helicase

It is known that upon dsDNA stimulation, STING interacts with TBK1, and they could together be co-precipitated by dsDNA, which presumably binds a DNA sensor that is also associated with the STING-TBK1 complex (Sharma et al., 2011; Tanaka and Chen, 2012). To elucidate the precise role of BTK in STING signaling, we used 5′-biotinylated-AT5-ODN in a streptavidin

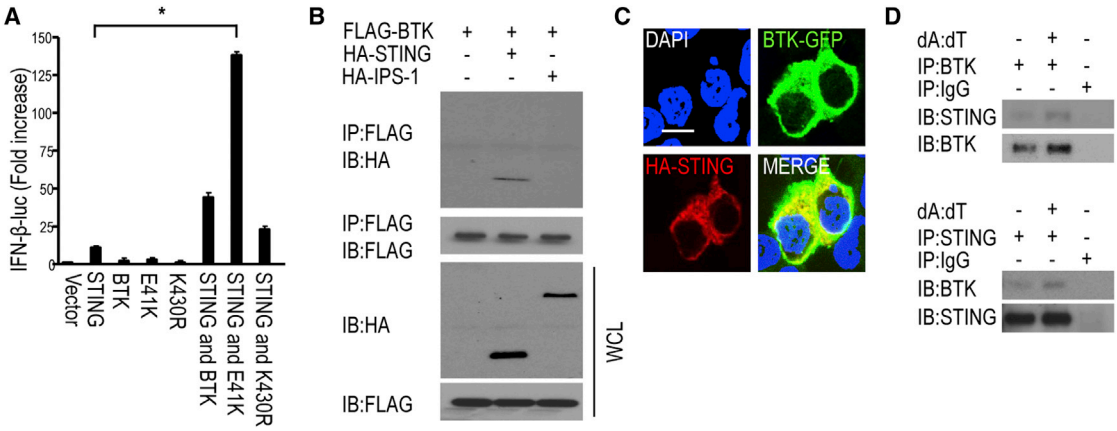

Figure 4. BTK Is a Component of STING Signaling

(A) BTK kinase activity synergizes with STING to induce *ifnb* promoter activity. HEK293T cells bearing IFN-β-promoter-luciferase (IFN-β-luc) plasmid as reporter and *Renilla* luciferase plasmid for normalization were transfected with empty vector or vectors expressing STING, BTK, constitutive-active (E41K) or kinase-dead (K430R) BTK, or both STING and BTK variants and assayed at 24 hr for luciferase activity. Data shown are representative of two independent experiments.

(B) BTK physically binds STING. HEK293T cells were co-transfected with FLAG-BTK and HA-STING or HA-IPS-1 plasmids. Whole cell lysates (WCLs) were immunoprecipitated (IP) with anti-FLAG and probed (IB) with anti-HA and anti-FLAG antibodies to examine BTK-STING interaction and expression of BTK, STING, and IPS-1.

(C) Confocal microscopy analysis of BTK and STING co-localization. HEK293T cells were co-transfected with GFP-tagged BTK and HA-tagged STING plasmids. STING expression was revealed with anti-HA antibody coupled to Alexa Fluor 594. DAPI staining revealed nuclei. Scale bar represents 10 μm.

(D) Endogenous BTK/STING interaction. Primary macrophages were nontreated or transfected with p(dA:dT) for 6 hr. BTK was IP to examine STING association (top) and vice-versa, and STING was IP to examine BTK binding (bottom). Nonspecific IgG was used as IP control.

See also Figure S4.

pull-down assay to examine STING-TBK1 complex formation in WT and *btk*$^{-/-}$ cells (Figure 5A). In WT cells, TBK1 and STING co-precipitated with 5′-biotinylated but not with control 3′-biotinylated AT5-ODN, consistent with published data (Sharma et al., 2011). BTK also co-precipitated with the STING-TBK1 complex in agreement with our earlier finding of BTK-STING interaction (Figure 4B). In contrast, STING-TBK1 complex formation was abolished in the absence of BTK. Hence, BTK is required for STING-TBK1 complex formation upon cytosolic dsDNA recognition.

We therefore hypothesize that BTK might be needed to phosphorylate and activate DNA sensors that directly bind dsDNA. One candidate is the DEAD-box helicase DDX41 (Zhang et al., 2011). We examined whether BTK could bind DDX41. We co-expressed HA-tagged DDX41 and FLAG-tagged BTK in HEK293T cells and found the two proteins co-immunoprecipitated (Figure 5B). Confocal microscopy studies indicated that BTK and DDX41 co-localized in murine RAW264.7 macrophage cells transfected with p(dA:dT) or cyclic di-GMP or stimulated with DMXAA (Figure 5C). We also showed endogenous BTK and DDX41 interaction in WT macrophages transfected with p(dA:dT) (Figure 5D). Finally, we immunoprecipitated DDX41 from WT macrophages (Figure 5E) or RAW264.7 cells (Figure 5F) transfected with p(dA:dT) or cyclic di-GMP and found endogenous DDX41 to be tyrosine phosphorylated.

We next asked whether ligand-induced DDX41 phosphorylation was specifically mediated by BTK. We showed that DDX41 tyrosine phosphorylation was abolished when p(dA:dT)-transfected cells were pretreated with LFM-A13 but not DMSO (Figure 5G). To further examine whether other tyrosine kinase could phosphorylate DDX41, we overexpressed FLAG-tagged DDX41 alone or together with HA-tagged WT BTK, constitutive active (E41K) or kinase dead (K430R) BTK or Src-family kinase Lyn in HEK293T cells (Figure 5H). We found BTK to be autophosphorylated in cells expressing WT or constitutive-active BTK. Interestingly, precipitated DDX41 was found to be phosphorylated only in the presence of WT or constitutive-active BTK but not with kinase-dead BTK or Lyn. In vitro kinase assay using GST-purified BTK and DDX41 (Figure 5I, top) confirmed that BTK directly phosphorylated DDX41 and DDX41 phosphorylation did not occur with kinase-dead (K430R) BTK (Figure 5I, bottom). These data suggested that BTK specifically phosphorylated DDX41 rather than acted as an adaptor to recruit another kinase. Finally, we showed that BTK specifically phosphorylated DDX41 but not another DEAD-box helicase, DDX1 (Figure 5J). Taken together, the data indicated that BTK directly binds and phosphorylates DDX41.

We also examined cGAS that sense dsDNA and CDNs and triggered IFN-β synthesis via the production of a secondary metabolite, cGAMP that activates STING (Sun et al., 2013; Diner et al., 2013; Ablasser et al., 2013). We examined whether BTK could bind and phosphorylate cGAS. We co-expressed HA-tagged cGAS with FLAG-tagged BTK or FLAG-tagged STING as control in HEK293T cells and found that BTK and cGAS could co-immunoprecipitate (Figure S5A). We also tested whether cGAS could be phosphorylated by BTK by overexpressing FLAG-tagged cGAS alone or together with HA-tagged BTK in HEK293T cells. However, cGAS was not phosphorylated by BTK (Figure S5B).

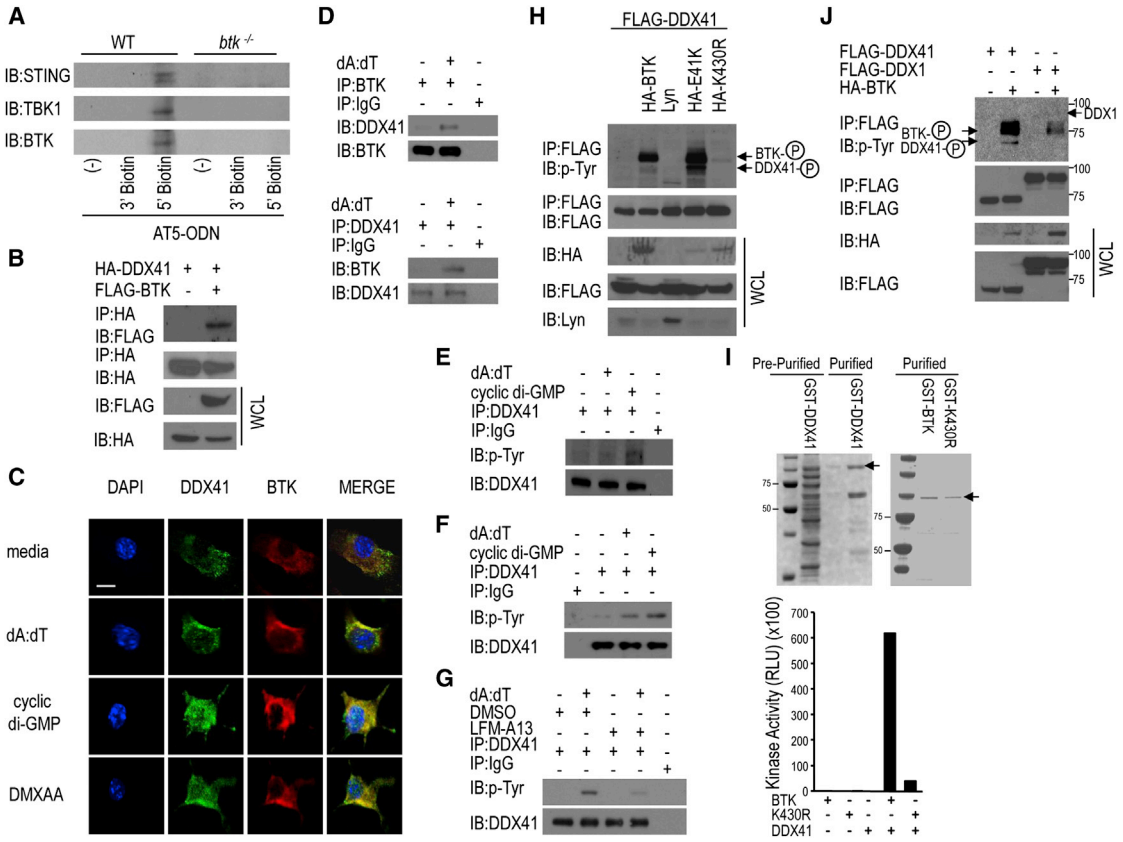

Figure 5. BTK Binds and Phosphorylates DDX41 Helicase

(A) Impaired STING-mediated intracellular DNA recognition in *btk*$^{-/-}$ cells. WT and *btk*$^{-/-}$ BMDMs were transfected with 5′- or 3′-biotinylated AT5-ODNs. Cell lysates were precipitated with Streptavidin and probed for STING, TBK1, and BTK association.

(B) BTK binds DDX41. Whole cell lysates (WCL) from HEK293T cells co-transfected with HA-DDX41 and FLAG-BTK were immunoprecipitated (IP) and immunoblotted (IB) to examine protein interaction and expression.

(C) Confocal microscopy analyses of BTK and DDX41 co-localization. RAW264.7 macrophage cells were untreated or transfected with p(dA:dT), cyclic di-GMP or stimulated with DMXAA and stained for BTK (red) and DDX41 (green) using fluorochrome-conjugated antibodies. Scale bar represents 10 μm.

(D) Endogenous BTK/DDX41 interaction. Primary macrophages were nontreated (m) or transfected for 6 hr with p(dA:dT). BTK was IP to examine DDX41 association (top) and vice versa; DDX41 was IP to examine BTK binding (bottom).

(E and F) DDX41 tyrosine phosphorylation in WT BMDMs (E) and RAW264.7 cells (F) transfected with p(dA:dT) and cyclic-di-GMP for 6 hr. DDX41 was IP and IB with anti-phosphotyrosine (pTyr) antibody. Anti-DDX41 blot served as loading controls.

(G) BTK activity is critical for DDX41 phosphorylation. RAW264.7 cells pretreated with DMSO or LFM-A13 for 1 hr and transfected with p(dA:dT) for 4 hr were examined for DDX41 phosphorylation as in (E). Nonspecific IgG controls were included in (D–G).

(H) BTK but not Lyn phosphorylates DDX41. HEK293T cells were transfected with FLAG-DDX41 and HA-BTK or Lyn or constitutive-active (E41K) or kinase-dead (K430R) HA-BTK plasmids. FLAG-tagged DDX41 was IP and IB with anti-pTyr antibody.

(I) In vitro kinase assay examining DDX41 phosphorylation by BTK. GST-tagged DDX41, BTK, and K430R-BTK were separated on SDS-PAGE gel, purified, and visualized by Coomassie-Brilliant Blue dye staining. Arrows depict positions of purified proteins (top). DDX41 phosphorylation by WT or (K430R) BTK was measured with ADP-Glo kinase assay. Data are plotted as nmol of phosphate transferred from ATP to DDX41 substrate (bottom panel).

(J) BTK phosphorylates DDX41 and not DDX1. HEK293T cells were transfected with FLAG-DDX41 or FLAG-DDX1 and with HA-BTK or without. FLAG-tagged DDX41 and DDX1 were IP and IB with 4G10 antibody. Protein expression of transfected plasmids were assayed as above.

See also Figure S5.

BTK Kinase and SH3/SH2 Domains Bind Respectively DEADc Domain of DDX41 and Transmembrane Region of STING

DDX41 binds STING upon ligand recognition via its DEAD-box (DEADc) domain and transmembrane region of STING (Zhang et al., 2011). To examine how BTK interacts with STING and DDX41, we generated full-length and mutants of BTK, DDX41, and STING (Figure 6A). We first studied domain interactions between BTK and DDX41 (Figure 6B). We found BTK to bind full-length DDX41 or DDX41 truncated at carboxyl-terminal (HELICc) or deleted of its helicase domain (ΔHELICc). However, BTK could not bind DDX41 lacking the DEADc domain (ΔDEADc).

Next, we examined DDX41 interaction with BTK (Figure 6C). DDX41 could bind full-length BTK or BTK deleted of its PH domain but not BTK deleted of kinase or combined kinase and SH3/SH2-interaction domains. Thus, the data indicated that BTK kinase domain associates with the DEADc domain of DDX41.

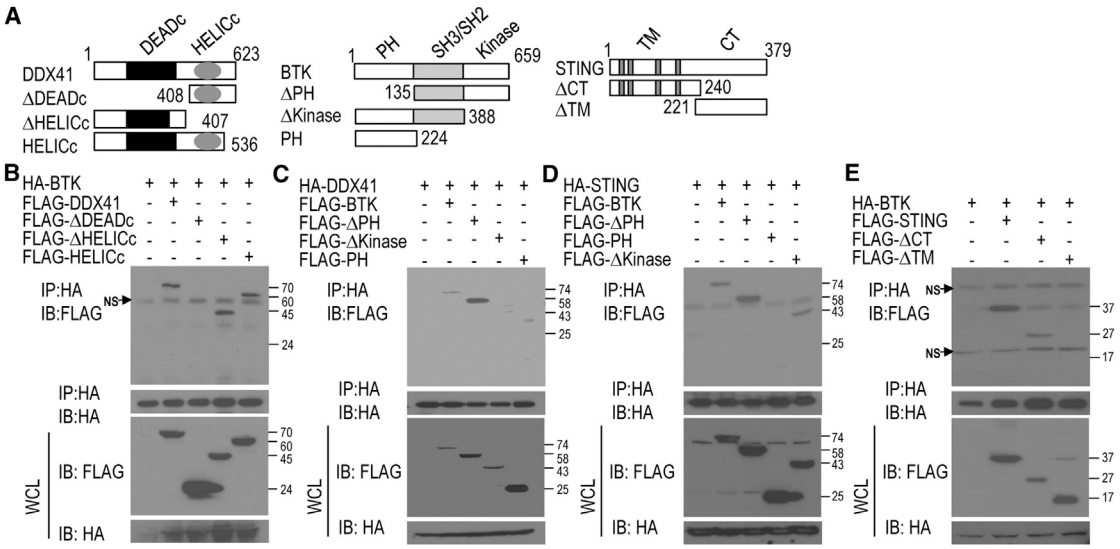

Figure 6. BTK/DDX41 and BTK/STING Domain Interactions

(A) Schematic representations of DDX41 (DEADc, Asp-Glu-Ala-Asp motif and HELICc, helicase C-terminal), BTK (PH, pleckstrin homology; SH2, Src Homology 2; and kinase), and STING (TM, transmembrane and CT, carboxyl terminal) and their various mutated forms. Numbers indicate amino acid positions.

(B) Analysis of BTK-DDX41 domain interactions. FLAG-tagged full-length DDX41 or mutants (HELICc, helicase truncation; ΔHELICc, helicase deletion; or ΔDEADc, DEADc deletion) were expressed with HA-BTK in HEK293T cells. BTK was IP and examined for full-length or mutant DDX41 binding using anti-FLAG antibody.

(C) Analysis of DDX41 binding to BTK domains. FLAG-tagged full-length BTK or mutants (ΔPH, PH domain deletion; ΔKinase, kinase deletion; or PH, SH3/SH2/Kinase domains deletion) were expressed with HA-tagged DDX41 in HEK293T cells. DDX41 was IP and examined for full-length or mutant BTK binding using anti-FLAG antibody.

(D) Analysis of STING-BTK domain interactions. HA-tagged full-length STING was expressed in HEK293T cells with FLAG-tagged full-length or mutants BTK. STING was IP and examined for binding of full-length or mutant BTK using anti-FLAG antibody.

(E) Analysis of BTK binding to STING domains. HEK293T cells were co-transfected with full-length HA-tagged BTK and FLAG-tagged full-length STING or mutant (ΔCT, C-terminal deletion; ΔTM, transmembrane deletion). HA-tagged BTK was IP and examined for STING domain interaction using anti-FLAG antibody. Data shown in (B–D) were representative of three independent experiments. Nonspecific (NS) bands were indicated. Size markers served as reference. Expression of transfected plasmids were assayed with whole cell lysates (WCLs).

Finally, we mapped the interacting domains of BTK and STING. Overexpression studies using full-length STING and various domains of BTK indicated that the PH and kinase domains of BTK were dispensable for binding STING and instead STING binds BTK through the latter's SH3/SH2-interaction domain (Figure 6D). On the other hand, reciprocal studies indicated that BTK binds STING deleted of its cytoplasmic but not transmembrane domains, suggesting that the transmembrane region of STING plays a critical role in binding BTK (Figure 6E).

Taken together, the data revealed that BTK kinase domain binds the DEADc domain of DDX41, while BTK's central SH3/SH2-interaction domain interacts with the transmembrane region of STING.

Tyr364 and Tyr414 of DDX41 Are Critical for Binding dsDNA and STING

Given that BTK kinase activity is required for IFN-β production (Figures 2H and 4A) and its kinase domain binds DDX41 (Figure 6C) and that BTK phosphorylates DDX41 (Figure 5I), we explored the significance of DDX41 phosphorylation by BTK. DDX41 binds dsDNA and STING (Zhang et al., 2011). Hence, we determined whether DDX41 phosphorylation by BTK is required for its binding of dsDNA. We transfected FLAG-tagged DDX41 and HA-tagged WT or kinase-dead BTK into HEK293T cells followed by precipitation of DDX41 with streptavidin-coupled magnetic beads after incubating cell lysates with 5′-biotinylated AT5-ODN. Interestingly, we found that only DDX41 co-expressed with WT but not kinase-dead BTK was phosphorylated and could be precipitated by 5′-biotinylated AT5-ODN (Figure 7A). These data suggested that DDX41 phosphorylation by BTK is required for its binding of dsDNA.

DDX41 has 16 tyrosine residues, and 3 of these (Y33, Y259, and Y414) were predicted by Netphos program to be phosphorylation sites (Table S1). To determine whether these tyrosine residues would be important for DDX41 sensing of dsDNA, we mutated them and four other tyrosine residues (Y279/280, Y340, and Y364) in the DEADc domain of DDX41 to phenylalanine given that this domain is important for binding dsDNA (Zhang et al., 2011). The site-directed mutants (SDM) of DDX41 were assessed for dsDNA binding using the 5′-biotinylated AT5-ODN precipitation assay. Interestingly, mutation of Tyr364 or Tyr414 to phenylalanine compromised the ability of DDX41 to bind dsDNA (Figure 7B), indicating that these two residues were individually critical for this function.

DDX41 binds STING upon ligand recognition (Zhang et al., 2011). We next asked whether this interaction would be affected in the absence of BTK. We transfected WT and *btk*$^{-/-}$

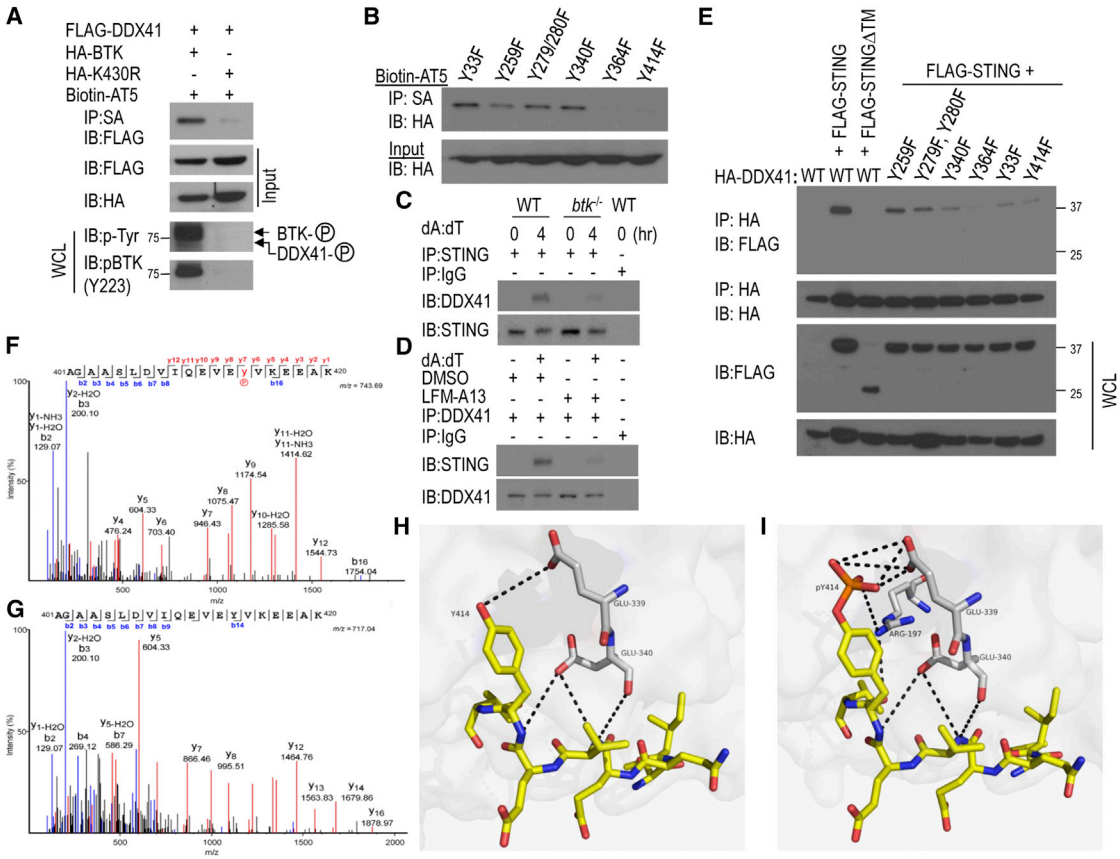

Figure 7. DDX41 Tyr364 and Tyr414 Are Required for Binding dsDNA and STING

(A) BTK kinase activity is required for DDX41 binding of dsDNA. Whole cell lysates (WCLs) from HEK293T cells co-transfected with FLAG-DDX41 and HA-tagged BTK or kinase-dead BTK (K430R) were incubated with 5′-biotinylated AT5-ODNs, precipitated with streptavidin and probed for DDX41 binding. Activation status of overexpressed BTK and DDX41 was examined using anti-pTyr and anti-phosphoBTK(Tyr223) antibodies.

(B) Tyr364 and Tyr414 are required for DDX41 binding of dsDNA. HEK293T cells were transfected with HA-tagged site-directed DDX41 Tyrosine (Y)-to-Phenylalanine (F) mutants. Cell lysates were incubated with 5′-biotinylated AT5-ODNs, precipitated with SA and probed for DDX41 binding using anti-HA antibody.

(C) BTK is required for DDX41 interaction with STING. WT and *btk*$^{-/-}$ BMDMs were stimulated with p(dA:dT) for 4 hr. Cell lysates were IP with anti-STING and probed with anti-DDX41 antibodies. The anti-STING blot served as loading control.

(D) BTK kinase activity is required for DDX41 and STING interaction. WT BMDMs were nontreated or treated with LFM-A13 and DDX41 was IP to probe for STING association. Nonspecific IgG Ab were included as controls in (C) and (D).

(E) Tyr364 and Tyr414 are critical for DDX41 binding to STING. HEK293T cells were transfected with HA-tagged DDX41 and FLAG-tagged STING or FLAG-tagged mutant STING deleted of transmembrane domain (ΔTM) or FLAG-tagged STING with various HA-tagged DDX41 Y-to-F mutants. Cell lysates were IP with anti-HA antibody for DDX41 and probed with anti-FLAG antibody to examine binding to STING. Expression of transfected plasmids (A, B, and E) was examined using whole cell lysates. Data shown were representative of three independent experiments.

(F and G) Mass spectrometry identification of DDX41 Tyr414-phosphorylation by BTK. (F) Fragment ions confirming the position of phosphorylated tyrosine residues. Matched fragment b- and y- ions are labeled as blue and red, respectively. LC-MS/MS spectrum of tyrosine phosphorylated 20-mer tryptic peptide T401-AGAASLDVIQEVEY(+79.97)VKEEAK-420 derived from DDX41, where "yⓅ" (red) indicates phosphorylated tyrosine at position Y414. The $[M+3H]^{3+}$ ion at *m/z* of 743.69 at retention time of 62.06 min was selected as precursor ion, one missed cleavage at K416. (G) LC-MS/MS spectrum of the $[M+3H]^{3+}$ precursor ion of unmodified 20-mer tryptic peptide of the same sequence (T401-AGAASLDVIQEVEYVKEEAK-420) derived from DDX41 at a *m/z* of 717.04 with retention time of 62.33 min.

(H and I) Computational modeling of DDX41 Tyr414 interaction with STING. Models of DDX41 peptide domain (amino acids 408–415) containing unmodified (H) and phosphorylated (I) Tyr414 docked onto transmembrane region of STING (amino acids 149–379). Carbons of DDX41 peptide are colored in yellow; carbons of STING are colored in gray. Y414 and pY414 of DDX41 and interacting residues of STING are labeled. Black dashed lines represent potential hydrogen bonds or salt bridges between DDX41 and STING. Images are made via PyMOL.

See also Figures S6 and S7 and Tables S1 and S2.

macrophages with p(dA:dT) and immunoprecipitated STING to examine DDX41 association. Our data indicated that DDX41 was not coupled to STING in the absence of BTK (Figure 7C). Furthermore, LFM-A13-inhibition study suggested that BTK kinase activity was required for DDX41 interaction with STING upon p(dA:dT) recognition (Figure 7D).

We hypothesized that the tyrosine residues critical for DDX41 to bind dsDNA might also be important for DDX41 to bind STING. Hence, we overexpressed WT and various SDM of DDX41 with STING in HEK293T cells and assayed their interactions (Figure 7E). As controls, we showed that WT DDX41 could bind full-length but not transmembrane-deleted STING. Mutations of Y259 and Y279/280 did not affect DDX41 binding to STING, while mutations of Y33 and Y340 appeared to weaken the interactions. Interestingly, mutations of Y364 and Y414 severely affected DDX41 binding to STING. These data are consistent with our earlier finding that Y364 and Y414 are critical for DDX41 recognition of ligands and with published data indicating that DDX41 binds STING after ligand sensing (Zhang et al., 2011).

Next, we employed high-resolution tandem mass spectrometry to identify BTK-mediated tyrosine phosphorylation sites within DDX41. We expressed FLAG-tagged DDX41 alone or with HA-tagged BTK in HEK293T cells and immunoprecipitated DDX41 to confirm its phosphorylation (Figure S6A). Upon SDS-PAGE separation, we excised the ~70 kDa DDX41 band (Figure S6B), digested it with trypsin in-gel, and analyzed it with nano-electrospray ionization-nano LC-orbitrap Fourier transform mass spectrometry. DDX41's identity was confirmed by peptide mapping with sequence coverage of 81%, and three tyrosine residues were revealed to be phosphorylated (Figure S7; Table S2), among them Y414 (Figures 7F and 7G).

Finally, we performed computational modeling using available crystal structures (Schütz et al., 2010; Shang et al., 2012) to gain insight to how Y414 phosphorylation might facilitate DDX41 and STING interaction. Our model indicated that DDX41 could not interact well with STING when Y414 was unmodified (Figure 7H). Y414 phosphorylation led to increased formation of hydrogen bonds and salt bridges with R197 and E339 on STING, hence promoting and enhancing interaction between the two proteins (Figure 7I). Incidentally, Y414 is proximal to the DEAD-box domain of DDX41, and R197 is in the transmembrane region of STING, the two domains that we and others (Zhang et al., 2011) had shown to be critical for STING and DDX41 interaction upon DDX41 ligand sensing.

DISCUSSION

We demonstrated here a role for BTK in STING-mediated IFN response. We showed that *btk*$^{-/-}$ cells were impaired in *ifnb* mRNA synthesis when challenged with pathogenic or infectious agents that activate STING signaling (Figure 1). These agents include the synthetic ligands p(dA:dT) and AT5-ODN, HSV-1 DNA, and AT-rich DNA from malarial parasites, CDNs, and the chemical agent DMXAA. Moreover, treatment of MEF and macrophages with these stimuli also led to BTK phosphorylation (Figures 2A–2G), which was indicative of its activation and therefore participation in STING signaling.

At the molecular level, BTK was shown to physically bind STING (Figures 4B–4D). This finding explains why the activation of TBK1 and IRF3, which are downstream of STING, was impaired in *btk*$^{-/-}$ cells treated with STING-activating stimuli (Figure 3). Detailed structural studies indicated that the SH3/SH2 interaction domain of BTK binds the transmembrane region of STING (Figures 6D and 6E). Thus, BTK might participate in STING signaling as an adaptor bridging STING to another molecule, be it the ligand sensor or other signaling moiety involved in the activation process. However, LFM-A13 inhibition experiments (Figure 2H) suggested that BTK functions more than an adaptor and its kinase activity is important for STING signaling. Thus, BTK likely phosphorylates a critical substrate. This was further supported by reconstitution (Figure 2I) and overexpression studies (Figure 4A), showing that constitutive-active but not kinase-dead BTK synergized with STING to drive *ifnb* promoter activity.

Our finding that BTK does not phosphorylate STING or TRIM56 (Figure S4) suggested that BTK likely phosphorylates another molecule that is very upstream in the signaling pathway. One possibility is that BTK phosphorylates the sensor of pathogenic agents. We established that BTK bound and phosphorylated DDX41 (Figure 5). On the other hand, BTK binds but does not phosphorylate cGAS (Figure S5).

The physiological relevance of DDX41 phosphorylation by BTK became apparent when site-directed mutagenesis experiments revealed Tyr414 of DDX41 as one of two residues critical for DDX41 binding of dsDNA (Figure 7B) and STING (Figure 7E). We show Tyr414 to be phosphorylated by BTK (Figures 7F and 7G). Tyr414 lies proximal to the DEAD-box and C-terminal helicase domain of DDX41 that is essential for high-affinity interaction with RNA/DNA substrate and for positioning nucleic acids for unwinding (Mallam et al., 2012). It is likely that Tyr414 phosphorylation by BTK enables DDX41 to bind dsDNA with higher affinity and strengthens DDX41 interaction with STING. Computational modeling suggested that Tyr414 phosphorylation increases the number of hydrogen bonds and salt bridges formed with R197 and E339 of STING (Figures 7H and 7I). R197 is in the transmembrane region of STING. The finding is consistent with our data and those of others, demonstrating interaction between DDX41 and transmembrane region of STING, and with finding that DDX41 binds STING upon ligand sensing (Zhang et al., 2011).

Tyr364 is the other residue critical for DDX41's function to bind dsDNA and STING (Figures 7B and 7E). It lies within the DEAD-box domain of DDX41, which is important for binding dsDNA (Zhang et al., 2011), CDNs (Parvatiyar et al., 2012), and transmembrane region of STING (Zhang et al., 2011). However, we could not detect Tyr364 phosphorylation by BTK. Nevertheless, Tyr364 is critical as its mutation to phenylalanine leads to defective binding of DDX41 to dsDNA and STING, probably due to conformational changes to DDX41 protein structure.

Taken together, a model emerges of how DDX41 senses dsDNA and other ligands and couples to STING to mediate IFN production. When cells were invaded by microbes, BTK is activated. The kinase domain of BTK binds the DEAD-box domain of DDX41, thereby allowing the kinase to phosphorylate DDX41. Phosphorylation of Tyr414 activates DDX41 and primes it to bind dsDNA and other ligands with high affinity and also strengthen and stabilizes DDX41 interaction with STING to activate TBK1/IRF3 leading to type 1 IFN production. Binding of dsDNA and transmembrane domain of STING is also mediated by the DEAD-box domain of DDX41 (Zhang et al., 2011), and Tyr364, proximal to the DEAD-box domain of DDX41, is critical for these functions. This model also explains the observation that DDX41 and STING could only

co-localize and be precipitated upon ligand activation (Zhang et al., 2011).

The role of STING as an adaptor to nucleate the formation of an IFN-inducing signalosome is further strengthened by our current finding, which adds BTK to the list of molecules shown to bind STING. It is known that STING binds TRIM56, which ubiquintylates and activates STING (Tsuchida et al., 2010). STING also binds TRIM32 (Zhang et al., 2012) and RIG-I (Nazmi et al., 2012) and TBK1 (Sharma et al., 2011; Tanaka and Chen, 2012; Zhang et al., 2012).

If BTK is critical in activating DDX41, what activates BTK when microbes invade the cells? We opined that when microbes first invade host cells, their PAMPS activate TLRs located on cell surface and in endosomes and subsequently BTK. We and others have shown that BTK participates in TLR-associated MyD88 and TRIF signaling (Lee et al., 2012; Liu et al., 2011). Activated BTK primes DDX41 and subsequently allows it to detect dsDNA and/or CDNs when these PAMPs appear in the cytosol. This tantalizing model can be readily tested.

EXPERIMENTAL PROCEDURES

Mice, Cells, and Plasmids

C57BL/6 and *btk*$^{-/-}$ mice were obtained from The Jackson Laboratory and bred in our facilities. Murine experiments were performed according to guidelines from the National Advisory Committee on Laboratory Animal Research. Bone marrow macrophages were differentiated as described (Boone et al., 2004). HEK293T cells were transfected with vectors encoding HA or FLAG-tagged genes using Lipofectamine2000 (Invitrogen). Cells were stimulated with p(dA:dT) (InvivoGen), p(I:C) (InvivoGen), DMXAA (Sigma), *E. coli* DNA (Sigma), HSV-1 DNA (ATCC), or cyclic di-GMP (Kerafast). Stimulants were given exogeneously or transfected with LyoVec (InvivoGen) or Lipofectamine 2000. For reconstitution experiments, HA-tagged *btk*, constitutive-active (E41K) and kinase-dead (K430R) *btk* were cloned into pBABE-Puro (Adgene) retroviral vector and checked by sequencing. Retroviruses were packaged using pCl-Neo vector (Adgene) and transduced into early passage *btk*$^{-/-}$ MEF in 4-μg/ml polybrene for 12 hr. Fresh culture media were introduced, and infected cells were selected in 2.5-μg/ml puromycin for 5 days prior to p(dA:dT) transfection.

Site-Directed Mutagenesis

DDX41 tyrosine-to-phenylalanine site-directed mutants were generated using QuickChange II Mutagenesis Kit (Stratagene). Primers used are in Supplemental Experimental Procedures (SEP).

Quantitative RT-PCR

Total RNA was extracted from WT and *btk*$^{-/-}$ BMDM and MEF using RNeasy Mini kit (QIAGEN) and synthesized into cDNA using Superscript II reverse transcriptase (Invitrogen). Quantitative RT-PCR was performed on Applied Biosystems 7500 real-time PCR system using specific primers listed in Supplemental Experimental Procedures.

Confocal Microscopy

Cells were washed twice with cold PBS containing 1% BSA/PBS and fixed with 4% paraformaldehyde/PBS for 20 min. After 10-min permeabilization (0.2% saponin-0.03M sucrose in 1% BSA/PBS) at room temperature, cells were washed twice with cold PBS, blocked with 5% BSA in PBS for 1 hr at room temperature, and incubated with primary antibodies at 4°C overnight. Slides were washed three times with 1% BSA/PBS, incubated 1 hr at room temperature with Anti-HA Alexa Fluor 594 anti-mouse IgG and chicken anti-rabbit Alexa Fluor 488 antibodies (Invitrogen/Molecular Probes), washed three times, mounted, and viewed with an Olympus confocal laser scanning microscope under 40× (normal) or 100× (oil) objective.

Strepavidin-Biotin DNA Binding Assay

Cells lysates were incubated with 1 μg of 3′- or 5′-biotinlynated AT5-ODN (using sequence as described (Sharma et al., 2011; IDT) and streptavidin-conjugated magnetic beads (50% w/v) for 2 hr. Lysates were washed with cold buffer (10-mM Tris-HCl, 1-mM EDTA, 2-M NaCl) and separated on a magnet before eluting with loading buffer containing SDS and boiled and run on 10% SDS-polyacrylamide gel.

Mass Spectrometry

Tandem mass spectrometry identification of DDX41 phosphorylation sites is detailed in Supplemental Experimental Procedures.

Statistics Analysis

Data are shown as mean ± SD; p values of less than 0.05 were considered statistically significant, *$p < 0.05$. Statistical differences were calculated with unpaired two-tailed Student's t test using prism software. Survival curves (Kaplan-Meyer plots) were compared using a log-rank test. Final mortality rates were compared with chi-square test.

SUPPLEMENTAL INFORMATION

Supplemental Information includes Supplemental Experimental Procedures, seven figures, and two tables and can be found with this article online at http://dx.doi.org/10.1016/j.celrep.2015.01.039.

AUTHOR CONTRIBUTIONS

K.-G.L., S.S.-Y.K., D.C.-C.V., M.M., P.B., X.B., N.A.P., C.L., and K.L performed research. B.S., L.R., and Y.I. advised on infection experiments. K.-P.L. conceptualized project and K.-G.L. and K.-P.L. analyzed data and wrote paper.

ACKNOWLEDGMENTS

We thank S.K. Ng for influenza virus infection, D.Y. Lee and laboratory members for discussion, and the Biopolis Resource Center for maintenance of mice.

Received: July 11, 2014
Revised: November 7, 2014
Accepted: January 15, 2015
Published: February 19, 2015

REFERENCES

Ablasser, A., Bauernfeind, F., Hartmann, G., Latz, E., Fitzgerald, K.A., and Hornung, V. (2009). RIG-I-dependent sensing of poly(dA:dT) through the induction of an RNA polymerase III-transcribed RNA intermediate. Nat. Immunol. *10*, 1065–1072.

Ablasser, A., Goldeck, M., Cavlar, T., Deimling, T., Witte, G., Röhl, I., Hopfner, K.P., Ludwig, J., and Hornung, V. (2013). cGAS produces a 2′-5′-linked cyclic dinucleotide second messenger that activates STING. Nature *498*, 380–384.

Barber, G.N. (2011). Innate immune DNA sensing pathways: STING, AIMII and the regulation of interferon production and inflammatory responses. Curr. Opin. Immunol. *23*, 10–20.

Blasius, A.L., and Beutler, B. (2010). Intracellular toll-like receptors. Immunity *32*, 305–315.

Boone, D.L., Turer, E.E., Lee, E.G., Ahmad, R.C., Wheeler, M.T., Tsui, C., Hurley, P., Chien, M., Chai, S., Hitotsumatsu, O., et al. (2004). The ubiquitin-modifying enzyme A20 is required for termination of Toll-like receptor responses. Nat. Immunol. *5*, 1052–1060.

Chiu, Y.H., Macmillan, J.B., and Chen, Z.J. (2009). RNA polymerase III detects cytosolic DNA and induces type I interferons through the RIG-I pathway. Cell *138*, 576–591.

Diner, E.J., Burdette, D.L., Wilson, S.C., Monroe, K.M., Kellenberger, C.A., Hyodo, M., Hayakawa, Y., Hammond, M.C., and Vance, R.E. (2013). The innate

immune DNA sensor cGAS produces a noncanonical cyclic dinucleotide that activates human STING. Cell Rep. *3*, 1355–1361.

Doyle, S.L., Jefferies, C.A., Feighery, C., and O'Neill, L.A. (2007). Signaling by Toll-like receptors 8 and 9 requires Bruton's tyrosine kinase. J. Biol. Chem. *282*, 36953–36960.

Gray, P., Dunne, A., Brikos, C., Jefferies, C.A., Doyle, S.L., and O'Neill, L.A. (2006). MyD88 adapter-like (Mal) is phosphorylated by Bruton's tyrosine kinase during TLR2 and TLR4 signal transduction. J. Biol. Chem. *281*, 10489–10495.

Hornung, V., Ablasser, A., Charrel-Dennis, M., Bauernfeind, F., Horvath, G., Caffrey, D.R., Latz, E., and Fitzgerald, K.A. (2009). AIM2 recognizes cytosolic dsDNA and forms a caspase-1-activating inflammasome with ASC. Nature *458*, 514–518.

Horwood, N.J., Page, T.H., McDaid, J.P., Palmer, C.D., Campbell, J., Mahon, T., Brennan, F.M., Webster, D., and Foxwell, B.M. (2006). Bruton's tyrosine kinase is required for TLR2 and TLR4-induced TNF, but not IL-6, production. J. Immunol. *176*, 3635–3641.

Ishikawa, H., Ma, Z., and Barber, G.N. (2009). STING regulates intracellular DNA-mediated, type I interferon-dependent innate immunity. Nature *461*, 788–792.

Jefferies, C.A., Doyle, S., Brunner, C., Dunne, A., Brint, E., Wietek, C., Walch, E., Wirth, T., and O'Neill, L.A. (2003). Bruton's tyrosine kinase is a Toll/interleukin-1 receptor domain-binding protein that participates in nuclear factor kappaB activation by Toll-like receptor 4. J. Biol. Chem. *278*, 26258–26264.

Khan, W.N., Alt, F.W., Gerstein, R.M., Malynn, B.A., Larsson, I., Rathbun, G., Davidson, L., Müller, S., Kantor, A.B., Herzenberg, L.A., et al. (1995). Defective B cell development and function in Btk-deficient mice. Immunity *3*, 283–299.

Lee, K.G., Xu, S., Wong, E.T., Tergaonkar, V., and Lam, K.P. (2008). Bruton's tyrosine kinase separately regulates NFkappaB p65RelA activation and cytokine interleukin (IL)-10/IL-12 production in TLR9-stimulated B Cells. J. Biol. Chem. *283*, 11189–11198.

Lee, K.G., Xu, S., Kang, Z.H., Huo, J., Huang, M., Liu, D., Takeuchi, O., Akira, S., and Lam, K.P. (2012). Bruton's tyrosine kinase phosphorylates Toll-like receptor 3 to initiate antiviral response. Proc. Natl. Acad. Sci. USA *109*, 5791–5796.

Liljeroos, M., Vuolteenaho, R., Morath, S., Hartung, T., Hallman, M., and Ojaniemi, M. (2007). Bruton's tyrosine kinase together with PI 3-kinase are part of Toll-like receptor 2 multiprotein complex and mediate LTA induced Toll-like receptor 2 responses in macrophages. Cell. Signal. *19*, 625–633.

Liu, X., Zhan, Z., Li, D., Xu, L., Ma, F., Zhang, P., Yao, H., and Cao, X. (2011). Intracellular MHC class II molecules promote TLR-triggered innate immune responses by maintaining activation of the kinase Btk. Nat. Immunol. *12*, 416–424.

Mallam, A.L., Del Campo, M., Gilman, B., Sidote, D.J., and Lambowitz, A.M. (2012). Structural basis for RNA-duplex recognition and unwinding by the DEAD-box helicase Mss116p. Nature *490*, 121–125.

Matsuda, T., Takahashi-Tezuka, M., Fukada, T., Okuyama, Y., Fujitani, Y., Tsukada, S., Mano, H., Hirai, H., Witte, O.N., and Hirano, T. (1995). Association and activation of Btk and Tec tyrosine kinases by gp130, a signal transducer of the interleukin-6 family of cytokines. Blood *85*, 627–633.

Mills, E., Pultz, I.S., Kulasekara, H.D., and Miller, S.I. (2011). The bacterial second messenger c-di-GMP: mechanisms of signalling. Cell. Microbiol. *13*, 1122–1129.

Mohamed, A.J., Yu, L., Bäckesjö, C.M., Vargas, L., Faryal, R., Aints, A., Christensson, B., Berglöf, A., Vihinen, M., Nore, B.F., and Smith, C.I. (2009). Bruton's tyrosine kinase (Btk): function, regulation, and transformation with special emphasis on the PH domain. Immunol. Rev. *228*, 58–73.

Nazmi, A., Mukhopadhyay, R., Dutta, K., and Basu, A. (2012). STING mediates neuronal innate immune response following Japanese encephalitis virus infection. Sci Rep *2*, 347.

Onomoto, K., Yoneyama, M., and Fujita, T. (2007). Regulation of antiviral innate immune responses by RIG-I family of RNA helicases. Curr. Top. Microbiol. Immunol. *316*, 193–205.

Opitz, B., Rejaibi, A., Dauber, B., Eckhard, J., Vinzing, M., Schmeck, B., Hippenstiel, S., Suttorp, N., and Wolff, T. (2007). IFNbeta induction by influenza A virus is mediated by RIG-I which is regulated by the viral NS1 protein. Cell. Microbiol. *9*, 930–938.

Parvatiyar, K., Zhang, Z., Teles, R.M., Ouyang, S., Jiang, Y., Iyer, S.S., Zaver, S.A., Schenk, M., Zeng, S., Zhong, W., et al. (2012). The helicase DDX41 recognizes the bacterial secondary messengers cyclic di-GMP and cyclic di-AMP to activate a type I interferon immune response. Nat. Immunol. *13*, 1155–1161.

Prantner, D., Perkins, D.J., Lai, W., Williams, M.S., Sharma, S., Fitzgerald, K.A., and Vogel, S.N. (2012). 5,6-Dimethylxanthenone-4-acetic acid (DMXAA) activates stimulator of interferon gene (STING)-dependent innate immune pathways and is regulated by mitochondrial membrane potential. J. Biol. Chem. *287*, 39776–39788.

Sato, S., Katagiri, T., Takaki, S., Kikuchi, Y., Hitoshi, Y., Yonehara, S., Tsukada, S., Kitamura, D., Watanabe, T., Witte, O., and Takatsu, K. (1994). IL-5 receptor-mediated tyrosine phosphorylation of SH2/SH3-containing proteins and activation of Bruton's tyrosine and Janus 2 kinases. J. Exp. Med. *180*, 2101–2111.

Schütz, P., Karlberg, T., van den Berg, S., Collins, R., Lehtiö, L., Högbom, M., Holmberg-Schiavone, L., Tempel, W., Park, H.W., Hammarström, M., et al. (2010). Comparative structural analysis of human DEAD-box RNA helicases. PLoS ONE *5*, 5.

Shang, G., Zhu, D., Li, N., Zhang, J., Zhu, C., Lu, D., Liu, C., Yu, Q., Zhao, Y., Xu, S., and Gu, L. (2012). Crystal structures of STING protein reveal basis for recognition of cyclic di-GMP. Nat. Struct. Mol. Biol. *19*, 725–727.

Sharma, S., DeOliveira, R.B., Kalantari, P., Parroche, P., Goutagny, N., Jiang, Z., Chan, J., Bartholomeu, D.C., Lauw, F., Hall, J.P., et al. (2011). Innate immune recognition of an AT-rich stem-loop DNA motif in the Plasmodium falciparum genome. Immunity *35*, 194–207.

Stein, S.C., Lam, E., and Falck-Pedersen, E. (2012). Cell-specific regulation of nucleic acid sensor cascades: a controlling interest in the antiviral response. J. Virol. *86*, 13303–13312.

Sun, L., Wu, J., Du, F., Chen, X., and Chen, Z.J. (2013). Cyclic GMP-AMP synthase is a cytosolic DNA sensor that activates the type I interferon pathway. Science *339*, 786–791.

Takaoka, A., Wang, Z., Choi, M.K., Yanai, H., Negishi, H., Ban, T., Lu, Y., Miyagishi, M., Kodama, T., Honda, K., et al. (2007). DAI (DLM-1/ZBP1) is a cytosolic DNA sensor and an activator of innate immune response. Nature *448*, 501–505.

Takeuchi, O., and Akira, S. (2009). Innate immunity to virus infection. Immunol. Rev. *227*, 75–86.

Tanaka, Y., and Chen, Z.J. (2012). STING specifies IRF3 phosphorylation by TBK1 in the cytosolic DNA signaling pathway. Sci. Signal. *5*, ra20.

Tsuchida, T., Zou, J., Saitoh, T., Kumar, H., Abe, T., Matsuura, Y., Kawai, T., and Akira, S. (2010). The ubiquitin ligase TRIM56 regulates innate immune responses to intracellular double-stranded DNA. Immunity *33*, 765–776.

Unterholzner, L., Keating, S.E., Baran, M., Horan, K.A., Jensen, S.B., Sharma, S., Sirois, C.M., Jin, T., Latz, E., Xiao, T.S., et al. (2010). IFI16 is an innate immune sensor for intracellular DNA. Nat. Immunol. *11*, 997–1004.

Zhang, Z., Yuan, B., Bao, M., Lu, N., Kim, T., and Liu, Y.J. (2011). The helicase DDX41 senses intracellular DNA mediated by the adaptor STING in dendritic cells. Nat. Immunol. *12*, 959–965.

Zhang, J., Hu, M.M., Wang, Y.Y., and Shu, H.B. (2012). TRIM32 protein modulates type I interferon induction and cellular antiviral response by targeting MITA/STING protein for K63-linked ubiquitination. J. Biol. Chem. *287*, 28646–28655.

Zhang, Z., Bao, M., Lu, N., Weng, L., Yuan, B., and Liu, Y.J. (2013). The E3 ubiquitin ligase TRIM21 negatively regulates the innate immune response to intracellular double-stranded DNA. Nat. Immunol. *14*, 172–178.